Light shifts and electric dipole matrix elements in Ba^+ and Ra^+

B. K. Sahoo, L. W. Wansbeek, K. Jungmann, and R. G. E. Timmermans
KVI, University of Groningen, NL-9747 AA Groningen, The Netherlands
(Received 26 March 2009; published 27 May 2009)

We present an analysis of the recent measurements of the light-shift ratio in Ba^+ at two different wavelengths that enables us to reduce the uncertainty of the largest $E1$ dipole matrix elements of Ba^+. These matrix elements are, for instance, of interest for the proposed parity-nonconservation (PNC) experiment in Ba^+. We show that a new measurement of the light-shift ratio in Ba^+ at a wavelength of 350 nm could further reduce the uncertainty of the (for PNC studies most important) $\langle 5D_{3/2}||D||6P_{1/2}\rangle$ matrix element. Finally, as groundwork for the planned PNC experiment at KVI, we present relativistic coupled-cluster calculations of the $E1$ matrix elements for Ra^+, and investigate the potential of similar light-shift ratio measurements in this ion.

DOI: 10.1103/PhysRevA.79.052512 PACS number(s): 32.10.Dk, 42.50.Hz, 31.15.bw

I. INTRODUCTION

Singly ionized barium (Ba^+) and radium (Ra^+) have been proposed as candidates for parity-nonconservation (PNC) experiments [1–3]. These ions are also suitable for atomic clock experiments [4]. Accurate determination of the electric dipole ($E1$) matrix elements is essential in achieving sub-1% PNC amplitudes. In the sum-over-the-states approach, the $E1_{\mathrm{PNC}}$ amplitude for the $7S_{1/2}\rightarrow 6D_{3/2}$ transition in Ra^+ is written as

$$E1_{\mathrm{PNC}} = \sum_{n=2}^{\infty}\left[\frac{\langle 7S_{1/2}||H^{\mathrm{PNC}}||nP_{1/2}\rangle\langle nP_{1/2}||D||6D_{3/2}\rangle}{E_{7S_{1/2}}-E_{nP_{1/2}}} + \frac{\langle 7S_{1/2}||D||nP_{3/2}\rangle\langle nP_{3/2}||H^{\mathrm{PNC}}||6D_{3/2}\rangle}{E_{6D_{3/2}}-E_{nP_{3/2}}}\right],$$

where H^{PNC} is the PNC Hamiltonian, D is the dipole operator, and E_i is the energy of state i. As shown in Ref. [3], by far the largest contribution to this sum is from the intermediate $7P_{1/2}$ state. This state contributes around 111%, while the second largest contributions are from the core orbitals $5P_{3/2}$ and $6P_{3/2}$ that contribute some 15% and 9%, respectively. This means that being able to accurately calculate the $\langle 7P_{1/2}||D||6D_{3/2}\rangle$ in Ra^+ (and the corresponding $6P_{1/2}$ matrix element in Ba^+ [5]) is especially desirable. The $E1$ matrix elements are also crucial in determining the dipole polarizabilities which are required to estimate shifts due to (stray) electric fields present in the experiments [6].

There is no direct method to measure $E1$ matrix elements, but they can be derived from a combination of branching ratio and lifetime measurements. If there are, however, two or more strong decay channels from a state, it is not possible to estimate the $E1$ matrix elements precisely. For instance, the available branching ratios [7–9] and lifetime [10–12] measurements of the first excited P states of Ba^+ do not enable an accurate determination of the $E1$ matrix elements. For Ra^+ no laser-spectroscopy experiments have been carried out yet.

The $E1$ matrix elements can be calculated to accurately using a modern-day many-body method. Since Ba^+ and Ra^+ are heavy systems, the electron correlation and relativistic effects are large. A variety of relativistic many-body methods have already been employed to calculate the $E1$ matrix elements for Ba^+ and Ra^+ [13–17]. The results obtained in these calculations, however, differ significantly in some cases, while for the proposed PNC experiments a sub-1% accuracy is needed. In this work, we have employed the relativistic coupled-cluster (RCC) method to calculate the pertinent $E1$ matrix elements in Ba^+ and Ra^+.

It was proposed recently [18] that the measurement of the ratio of two light shifts (ac Stark shifts) could provide a way to accurately determine $E1$ matrix elements. By choosing a particular wavelength, the contribution from a specific matrix element to the light shift becomes relatively large. By taking the ratio of the differential light shift of two different states, the uncertainty in the laser light intensity is eliminated. Recently, such a light-shift ratio measurement in Ba^+ at two different wavelengths was performed [19,20]. In Ref. [20] the outcomes of the measurements were used to calculate two $E1$ matrix elements; a more sophisticated analysis is underway. In this paper, we present a different analysis of these measurements. We show how they can be used to reduce the uncertainty of the most relevant $E1$ matrix elements of Ba^+. We also calculate the wavelength at which a new light-shift ratio measurement would be the most informative for a PNC experiment. Finally, we turn our attention to Ra^+. Using coupled-cluster calculations of the $E1$ matrix elements, we analyze if a similar light-shift ratio measurement in Ra^+ is useful, and what the optimal wavelength for such a measurement would be.

II. LIGHT-SHIFT RATIO

The energy shift of an atomic state $|\gamma,J,m\rangle$ due to nonresonant ac light in an average period of light oscillations, neglecting the mixing of the magnetic sublevels, is given by [20]

$$\Delta E(\gamma,J,m) = -\frac{\alpha_0}{2}|\mathbf{E}|^2 - i\frac{\alpha_1}{2}m(i|\mathbf{E}^*\times\mathbf{E}|) - \frac{\alpha_2}{2}\left(\frac{3m^2-J(J+1)}{J(2J-1)}\right)\frac{3E_z^2-|\mathbf{E}|^2}{2}. \quad (2.1)$$

This is the ac Stark or light shift. In this expression, J represents the total angular momentum, m is the magnetic quantum number, and γ is an additional index representing other

relevant quantum numbers. **E** is the applied electric field vector, and E_z is its magnitude in the z direction. α_0, α_1, and α_2 are the scalar, vector, and tensor polarizabilities of the state $|\gamma,J,m\rangle$. They are given by [21,22]

$$\alpha_0(\gamma,J) = -\frac{2}{3[J]}\sum_{K\neq J}\frac{E_J - E_K}{(E_J-E_K)^2-\omega^2} \times |\langle\gamma' K||D||\gamma J\rangle|^2\phi_0(J,K),$$

$$\alpha_1(\gamma,J) = -\frac{1}{[J]}\sum_{K\neq J}\frac{\omega}{(E_J-E_K)^2-\omega^2} \times |\langle\gamma' K||D||\gamma J\rangle|^2\phi_1(J,K),$$

$$\alpha_2(\gamma,J) = -\frac{2}{3[J]}\sum_{K\neq J}\frac{E_J - E_K}{(E_J-E_K)^2-\omega^2} \times |\langle\gamma' K||D||\gamma J\rangle|^2\phi_2(J,K). \quad (2.2)$$

Here D is the dipole operator and $[J]=2J+1$ is the degeneracy factor. $|\gamma',K\rangle$ represents states of opposite parity to $|\gamma,J\rangle$, matrix elements with double bars are reduced matrices, E_i is the energy of state i in the absence of an external electric field, and ω is the frequency of the applied electric field. The angular factors $\phi_i(J,K)$ $(i=0,1,2)$ are defined as

$$\phi_0(J,K) = \delta_{J-1,K} + \delta_{J,K} + \delta_{J+1,K},$$

$$\phi_1(J,K) = -\frac{1}{J}\delta_{J-1,K} - \frac{1}{J(J+1)}\delta_{J,K} + \frac{1}{J+1}\delta_{J+1,K},$$

$$\phi_2(J,K) = -\delta_{J-1,K} + \frac{2J-1}{J+1}\delta_{J,K} - \frac{J(2J-1)}{(J+1)(2J+3)}\delta_{J+1,K}. \quad (2.3)$$

When the applied electric field is circularly polarized and aligned with the magnetic field, the vector shift is at its maximum value. Also, we can see from Eq. (2.1) that the differential light shift between $\pm m$ Zeeman states, $\Delta E(\gamma,J,m) - \Delta E(\gamma,J,-m)$, depends only on the vector polarizability α_1. Further, if we were to take the ratio of the differential light shifts of two different states, we see that the dependence on the electric field cancels.

Hence, we define [18–20]

$$\mathcal{R} \equiv \frac{\Delta E_{6S_{1/2},m=1/2} - \Delta E_{6S_{1/2},m=-1/2}}{\Delta E_{5D_{3/2},m=1/2} - \Delta E_{5D_{3/2},m=-1/2}},$$

which is the ratio of the differential light shifts of the $6S_{1/2}$ and $5D_{3/2}$ states of Ba^+. Using Eq. (2.1) this can be written as

$$\mathcal{R} = \frac{\alpha_1(6S_{1/2})}{\alpha_1(5D_{3/2})},$$

where we slightly rewrite the vector polarizability as

$$\alpha_1(\gamma,J) = -\frac{1}{2[J]}\sum_{K\neq J}\left(\frac{1}{\Delta\omega_{JK}-\omega} - \frac{1}{\Delta\omega_{JK}+\omega}\right) \times |\langle\gamma' K||D||\gamma J\rangle|^2\phi_1(J,K). \quad (2.4)$$

The relative minus sign of the two terms between brackets in Eq. (2.4) disagrees with Refs. [18–20]; cf. Ref. [21].

Once the $E1$ matrix elements are known, calculating the lifetime of a state is straightforward. The probability coefficient $A^{E1}_{f\to i}[s^{-1}]$ for an $E1$-induced decay between initial state i and final state f is given by

$$A^{E1}_{f\to i} = \frac{2.026\ 13\times 10^{21}}{\lambda(2J_f+1)}|\langle f||D||i\rangle|^2.$$

To find the total decay rate out of state i, one simply adds the different decay channels. For the $nP_{1/2}$ and the $nP_{3/2}$ states ($n=6$ and 7 for Ba^+ and Ra^+, respectively), we have

$$A^{E1}_{nP_{1/2}} = A_{nP_{1/2}\to(n-1)D_{3/2}} + A_{nP_{1/2}\to nS_{1/2}},$$

$$A^{E1}_{nP_{3/2}} = A_{nP_{3/2}\to(n-1)D_{3/2}} + A_{nP_{3/2}\to(n-1)D_{5/2}} + A_{nP_{3/2}\to nS_{1/2}}.$$

The lifetimes are given by

$$\tau_{nP_{1/2}} = [A^{E1}_{nP_{1/2}}]^{-1},$$

$$\tau_{nP_{3/2}} = [A^{E1}_{nP_{3/2}}]^{-1}.$$

III. DIPOLE MATRIX ELEMENTS OF THE BARIUM ION

To calculate the wave functions of Ba^+ and Ra^+, we have employed the RCC theory for the Dirac-Coulomb Hamiltonian. We take into account single (S) and double (D) excitations, along with important triple (T) excitations. This is called the CCSD(T) method. As shown in earlier works [23], contributions from higher triple and quadrupole excitations arise through the nonlinear terms in the CCSD(T) method. The contributions from these nonlinear terms to the various properties in heavy systems are significant, which means that the often-used linear approximation does not work well for heavy systems.

In order to make an estimate of the errors of the calculated $E1$ matrix elements, we used two different gauges for the calculation, the length and the velocity gauges. We took the difference in outcome between these two calculation methods as an estimate of the lower limit of the error. For the D and F states, however, the velocity gauge did not converge well. Consequently, for these states we took the difference between the CCSD, i.e., without triple excitations, and the CCSD(T) calculation as the error.

We present our results for the dipole matrix elements of Ba^+ in Table I. Also shown are the results from other groups. As the table shows, the different calculations disagree due to the different many-body theories used. We will briefly discuss the main differences.

Gopakumar *et al.* [14] used a method similar to ours. They, however, used a mix of numerical orbitals from

TABLE I. Absolute magnitudes of the reduced electric dipole matrix elements in Ba^+. Estimated error bars are given inside parentheses.

Transition	Present	Ref. [13]	Ref. [14]	Ref. [15]	Ref. [16]
$6P_{1/2}\rightarrow 6S_{1/2}$	3.36(1)	3.310	3.3266	3.3357	3.300
$7P_{1/2}\rightarrow 6S_{1/2}$	0.10(1)	0.099	0.1193	0.0621	
$8P_{1/2}\rightarrow 6S_{1/2}$	0.11(5)	0.115	0.4696		
$6P_{3/2}\rightarrow 6S_{1/2}$	4.73(3)	4.674	4.6982	4.7065	4.658
$7P_{3/2}\rightarrow 6S_{1/2}$	0.17(5)	0.035	0.3610	0.0868	
$8P_{3/2}\rightarrow 6S_{1/2}$	0.11(5)	0.073	0.5710		
$6P_{1/2}\rightarrow 7S_{1/2}$	2.44(4)	2.493	2.3220		
$6P_{1/2}\rightarrow 8S_{1/2}$	0.66(5)	0.705	0.7283		
$6P_{3/2}\rightarrow 7S_{1/2}$	3.80(2)	3.882	3.6482		
$6P_{3/2}\rightarrow 8S_{1/2}$	0.97(5)	1.025	1.0518		
$6P_{1/2}\rightarrow 5D_{3/2}$	3.11(3)	3.055	2.9449		3.009
$7P_{1/2}\rightarrow 5D_{3/2}$	0.28(2)	0.261	0.3050		
$8P_{1/2}\rightarrow 5D_{3/2}$	0.13(2)	0.119	0.1121		
$6P_{3/2}\rightarrow 5D_{3/2}$	1.34(2)	1.334	1.2836		1.312
$7P_{3/2}\rightarrow 5D_{3/2}$	0.16(1)	1.472	0.1645		
$8P_{3/2}\rightarrow 5D_{3/2}$	0.07(2)	0.070	0.0650		
$4F_{5/2}\rightarrow 5D_{3/2}$	3.75(11)				
$5F_{5/2}\rightarrow 5D_{3/2}$	1.59(8)				
$6F_{5/2}\rightarrow 5D_{3/2}$	0.17(2)				
$6P_{3/2}\rightarrow 5D_{5/2}$	4.02(7)	4.118	3.9876		4.057
$7P_{3/2}\rightarrow 5D_{5/2}$	0.46(1)	0.432	0.4788		
$8P_{3/2}\rightarrow 5D_{5/2}$	0.21(2)	0.206	0.1926		
$4F_{5/2}\rightarrow 5D_{5/2}$	1.08(4)				
$5F_{5/2}\rightarrow 5D_{5/2}$	0.45(7)				
$6F_{5/2}\rightarrow 5D_{5/2}$	0.15(2)				
$4F_{7/2}\rightarrow 5D_{5/2}$	4.84(5)				
$5F_{7/2}\rightarrow 5D_{5/2}$	2.47(6)				
$6F_{7/2}\rightarrow 5D_{5/2}$	1.04(7)				
$6P_{1/2}\rightarrow 6D_{3/2}$	4.89(10)				
$6P_{1/2}\rightarrow 7D_{3/2}$	1.50(8)				
$6P_{3/2}\rightarrow 6D_{3/2}$	2.33(7)				
$6P_{3/2}\rightarrow 7D_{3/2}$	0.67(4)				
$6P_{3/2}\rightarrow 6D_{5/2}$	6.91(21)				
$6P_{3/2}\rightarrow 7D_{5/2}$	2.01(5)				

GRASP [24], and Gaussian-type analytical orbitals (GTOs). In the present work, we use purely analytical GTOs. Das [25] also truncated at the effective one-body terms, while we consider higher-order terms. The main difference between the method of Dzuba *et al.* [13] and our method was in detail discussed in Ref. [14]. Briefly, Dzuba *et al.* [13] employed the Green's-function technique, also an all-order perturbative method using purely analytical orbitals. However, compared to this method, our RCC method incorporates more excitations through its nonlinear terms.

Iskrenova-Tchoukova and Safronova [15] used the linearized CCSD method, with important triple excitations. The orbitals have been constructed using B splines. As discussed above, the nonlinear terms can incorporate higher-order correlation effects, which can contribute significantly in these heavy systems [23]. Also, the procedure we use to incorporate partial triple excitations differs from the method used in Ref. [15]. We consider effects of partial triple excitations by estimating at each iteration their contribution to the energy of the corresponding valence state. Next, we solve the CCSD method amplitudes self-consistently, while Ref. [15] includes them directly in the amplitude-determining equations. Guet and Johnson [16] used the relativistic many-body method to second order [MBPT(2) method], using a B-spline basis.

IV. ANALYSIS OF THE LIGHT-SHIFT METHOD FOR THE BARIUM ION

Table II shows an overview of all the experimental values for the matrix elements we could find in the literature. In the rightmost column, the weighted averages of the experimental data are shown. Using these data, we have calculated the differential light shifts of the $m=1/2$ and the $m=-1/2$ levels of the $6S_{1/2}$ and $5D_{3/2}$ states. The results are shown in Fig. 1. The plot starts at 250 nm, while all the transitions to the higher-lying states are at lower wavelengths. Since we are not interested in these transitions, we left them out of the plot. As the plot shows, the light shift of the D state goes through zero at a wavelength of 590 nm. Clearly visible in the plot are the peaks at the different transitions. For the $6S_{1/2}$ state, these are the transitions to the $6P_{3/2}$ state at 456 nm, and the $6P_{1/2}$ state at 494 nm. For the $5D_{3/2}$ state there is at 230 nm, just outside the plot, the transition to the $4F_{5/2}$ state, at 586 nm the transition to the $6P_{3/2}$ state, and at 650 nm the transition to the $6P_{1/2}$ state. Shown in the plot are the contributions from these different states to the D-state light shift.

Next, we write the ratio of the differential light shifts of the above states in the sum-over-the-states approach, where we take the $6P_{1/2}$, $7P_{1/2}$, $8P_{1/2}$, $6P_{3/2}$, $7P_{3/2}$, $8P_{3/2}$, $4F_{5/2}$, $5F_{5/2}$, and $6F_{5/2}$ states into account as the intermediate states. Using the MBPT(2) method we estimate the total contribution of the thus neglected core (C), core-valence (CV), and higher-lying valence (V) states. The largest contribution, more than 90%, to the core, core valence, and valence (CCVV) total comes from the core states. Further, we found that for energies lower than 0.13 Ry (corresponding to wavelengths higher than 350 nm), these contributions show almost perfect linear behavior in the frequency of the laser light. Looking at Eq. (2.2) this makes sense. For $\omega\rightarrow 0$ and the energy difference between the valence and the intermediate states (E_J-E_K) becoming larger, a linear dependence on ω emerges. Using these linear dependencies, $\mathcal{R}$ can be rewritten as

$$\mathcal{R}(\lambda)=2\frac{\displaystyle\sum_{i=1}^{6}\frac{a_i p_i^2}{(\lambda/\Delta\lambda_i)^2-1}-\left(\frac{\xi(6S_{1/2})}{\lambda}\right)^2}{\displaystyle\sum_{i=7}^{15}\frac{a_i p_i^2}{(\lambda/\Delta\lambda_i)^2-1}-\left(\frac{\xi(5D_{3/2})}{\lambda}\right)^2}, \tag{4.1}$$

where λ is the frequency of the laser field in nm, a_i are constants calculated using Eq. (2.3), p_i are the dipole matrix

TABLE II. Theoretical and experimental (absolute) values of the reduced dipole matrix elements of Ba^+.

Transition	$\Delta\lambda$ (nm)		Experimental values				
			Ref. [7]	Ref. [9]	Refs. [27,28]	Ref. [29]	Average
$6S_{1/2}$-$6P_{1/2}$	493.545	p_1	3.36(16)	3.36(12)	3.36(4)		3.36(4)
$6S_{1/2}$-$7P_{1/2}$	202.471	p_2			0.24(3)		0.24(3)
$6S_{1/2}$-$8P_{1/2}$	163.040	p_3			0.10(1)		0.10(1)
$6S_{1/2}$-$6P_{3/2}$	455.531	p_4	4.45(19)	4.69(16)	4.55(10)	4.72(4)	4.69(4)
$6S_{1/2}$-$7P_{3/2}$	199.952	p_5			0.33(4)		0.33(4)
$6S_{1/2}$-$8P_{3/2}$	162.200	p_6			0.15(2)		0.15(2)
$5D_{3/2}$-$6P_{1/2}$	649.869	p_7	3.03(9)	2.99(18)	2.90(9)		2.97(6)
$5D_{3/2}$-$7P_{1/2}$	224.638	p_8			0.42(11)		0.42(11)
$5D_{3/2}$-$8P_{1/2}$	177.103	p_9			0.23(6)		0.23(6)
$5D_{3/2}$-$6P_{3/2}$	585.530	p_{10}	1.36(4)	1.38(9)	1.54(19)	1.349(36)	1.36(3)
$5D_{3/2}$-$7P_{3/2}$	221.545	p_{11}			0.19(5)		0.19(5)
$5D_{3/2}$-$8P_{3/2}$	176.175	p_{12}			0.10(3)		0.10(3)
$5D_{3/2}$-$4F_{5/2}$	230.496	p_{13}					
$5D_{3/2}$-$5F_{5/2}$	190.414	p_{14}					
$5D_{3/2}$-$6F_{5/2}$	167.451	p_{15}					
$\mathcal{R}(514.53)$							−12.07(33)
$\mathcal{R}(1111.68)$							0.495(46)

elements, and $\Delta\lambda_i$ are the corresponding frequency differences. The constants $\xi(6S_{1/2})$ and $\xi(5D_{3/2})$ give the CCVV contributions, and take values of $\xi(6S_{1/2}) \simeq 170.8$ and $\xi(5D_{3/2}) \simeq 136.8$. The energy differences $\Delta\lambda_i$ in Ba^+ are known to rather high precision [26], so we will take these values as given.

Figure 2 shows the light-shift ratios for Ba^+ calculated using Eq. (4.1) and the average experimental values from Table II. Clearly visible in the plot are the two peaks (infinities) corresponding to the $6S_{1/2} \leftrightarrow 6P_{1/2}$ and $6S_{1/2} \leftrightarrow 6P_{3/2}$ transitions. Since the transitions to the $5D_{3/2}$ states are in the denominator, we expect the ratio to go through zero in those points. This is indeed the case. Since the D-state shift goes through zero at 590 nm, an extra peak appears there.

By choosing a specific wavelength, the importance of a contribution from a particular state to the light-shift ratio can be maximized. Experimental values of this light-shift ratio can therefore be a powerful tool in the analysis of certain dipole matrix elements. In Ref. [20] such a measurement for $^{138}Ba^+$ was done, for two different wavelengths. The results were

$$\mathcal{R}(\lambda_1 = 514.53 \text{ nm}) = -11.494(13),$$

$$\mathcal{R}(\lambda_2 = 1111.68 \text{ nm}) = 0.4176(8).$$

The uncertainties in these measurements are at impressive 0.1% and 0.2%, respectively. These errors are sufficiently small to be neglected for our purpose. We will now use these results to put constraints on the values of the $E1$ matrix elements in Ba^+.

In the following, we use the shorthand notation p_i for the $E1$ dipole elements, where the numbering is shown in Table II. The values between brackets are the uncertainties, which we will interpret as $1\sigma_p$ values. Also shown in this table is the light-shift ratio calculated with Eq. (4.1), where we have used the theoretical values for the p_{13} matrix element and included the CCVV contribution.

We will now study what the experimentally determined light-shift ratios can say about the values and the uncertainties of the dipole matrix element. For the two wavelengths at which the experiments have been performed, and in view of the size of the different p_i, we focus on the parameters $p = \{p_1, p_4, p_7, p_{10}, p_{13}\}$. We have an initial set of values ($\bar{p}$), but we also have more information about these values, namely, two measurements of the light-shift ratio ($\mathcal{R}$). How does this extra information influence our data? This problem is conveniently addressed by using the properties of the conditional normal distribution. The details of the method are in the Appendix. As input for the initial values $\bar{p}$ we took the averaged experimental values; see Table II. For the experimentally unknown matrix element $p_{13} = \langle 5D_{3/2} || D || F_{5/2} \rangle$ we take our calculated value of 3.75, but we take a larger uncertainty of 0.5 to be on the safe side. This results in

$$p_1 = \langle 6S_{1/2} || D || 6P_{1/2} \rangle = 3.32(2) \quad [3.36(4)],$$

$$p_4 = \langle 6S_{1/2} || D || 6P_{3/2} \rangle = 4.70(3) \quad [4.69(4)],$$

$$p_7 = \langle 5D_{3/2} || D || 6P_{1/2} \rangle = 3.02(4) \quad [2.97(6)],$$

$$p_{10} = \langle 5D_{3/2} || D || 6P_{3/2} \rangle = 1.36(3) \quad [1.36(3)],$$

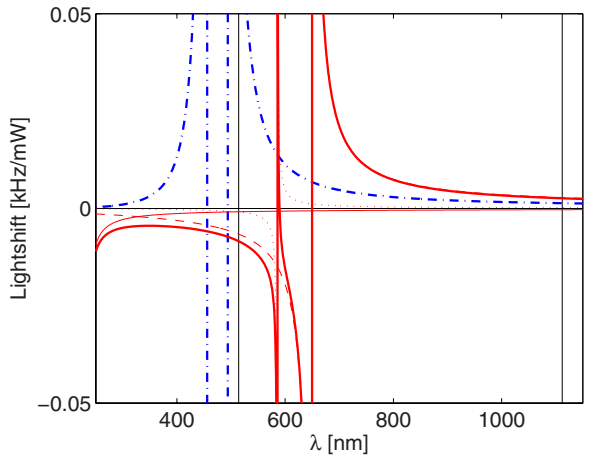

FIG. 1. (Color online) The differential light shifts between the $m_{1/2}$ and $m_{-1/2}$ states of the $6S_{1/2}$ (dash-dotted blue line) and $5D_{3/2}$ (thick solid red line) levels of Ba^+. We used the averaged experimental data from Table II and assumed a laser focused on a spot with radius of 50 μm. Also shown are the individual contributions from $\langle 5D_{3/2}||D||6P_{1/2}\rangle$ (dashed red line), $\langle 5D_{3/2}||D||6P_{3/2}\rangle$ (dotted red line), and $\langle 5D_{3/2}||D||4F_{5/2}\rangle$ (thin red line). The two vertical lines indicate the wavelengths at which the two experiments were performed.

$$p_{13} = \langle 5D_{3/2}||D||4F_{5/2}\rangle = 3.94(33) \quad [4.0(5)] \qquad (4.2)$$

for our recommended values for the matrix elements. Between the square brackets, the initial values and uncertainties are shown. We see that because of the two light-shift ratio measurements, the values of the dipole matrix elements have shifted. The largest shifts are in the p_1 and p_7 matrix elements, but the changes are not bigger than 1 standard deviation. As expected, the uncertainties in the matrix elements have decreased, except for the p_{10} element. The reason is that the sensitivity of the light-shift ratio at the experimental wavelengths to this matrix element is simply too small. Comparing to Table I, we conclude that in general the theoretical values for the matrix elements differ from these recommended values by at most 2 standard deviations. The outcome is rather insensitive to the starting value of the

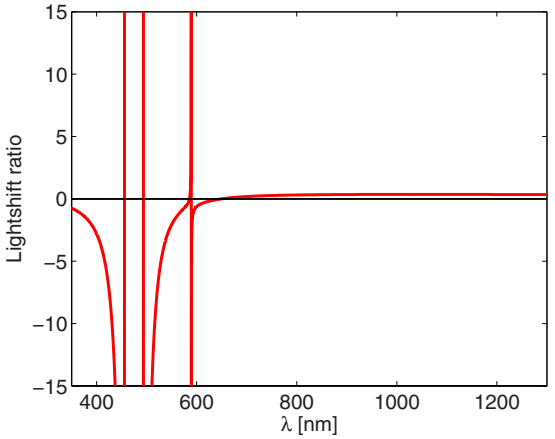

FIG. 2. (Color online) The light-shift ratios of Ba^+.

TABLE III. The lifetimes of the $6P_{1/2}$ and $5P_{3/2}$ states of Ba^+. The probability coefficients A are given in MHz, and the lifetimes in ns.

$6P_{1/2}$		$6P_{3/2}$	
$A(\rightarrow 6S_{1/2})$	92.9(1.1)	$A(\rightarrow 6S_{1/2})$	118.9(3.6)
$A(\rightarrow 5D_{3/2})$	33.4(1.1)	$A(\rightarrow 5D_{3/2})$	4.7(1)
		$A(\rightarrow 5D_{5/2})$	35.3(2.5)
$A^{E1}(6P_{1/2})$	126.3(1.6)	$A^{E1}(7P_{1/2})$	158.8(4.3)
$\tau(6P_{1/2})$	7.92(10)	$\tau(7P_{3/2})$	6.30(17)
Expt. [10]	7.92(8)	Expt. [11]	6.32(10)
Expt. [11]	7.90(10)	Expt. [12]	6.312(16)

(experimentally) unknown $p_{13}=\langle 5D_{3/2}||D||F_{5/2}\rangle$ matrix element. Varying p_{13} from 3.25 to 4.5 with an uncertainty of 0.5 gives for p_7 a range of 2.99(5)–3.04(5) and for its own value a range of 3.85(33)–4.30(33). p_1, p_4, and p_7 do not change.

The results in Eq. (4.2) differ from the findings of Ref. [20]. There the light-shift ratio equation and the two experimental results were used to solve for two of the unknown dipole matrix elements. The results were

$$p_7 = \langle 5D_{3/2}||D||6P_{1/2}\rangle = 3.14(8),$$

$$p_{13} = \langle 5D_{3/2}||D||4F_{5/2}\rangle = 4.36(36).$$

The reason for the discrepancy between this and our result lies again in the extra minus sign in Eq. (2.4) and the fact that we took CCVV contributions into account.

Using the values in Eq. (4.2), we can also calculate the lifetimes of the $6P_{1/2}$ and $6P_{3/2}$ states and compare them to experimental values. The lifetime of the $6P_{1/2}$ state only depends on p_1 and p_7. Therefore, from a PNC point of view, this lifetime is a good test of our method. The lifetime of the $6P_{3/2}$ state depends on p_4 and p_{10}, and on the matrix element $\langle 6D_{5/2}||D||6P_{3/2}\rangle$, which we take from Table I. The resulting lifetimes are given in Table III. The agreement between our results and the experimental values is very good.

A nice feature of our approach is that we can use it to find that wavelength at which a new measurement would give the largest decrease in the variance of the matrix elements. Suppose that before the measurement, we have a matrix S with the variances of the dipole matrix elements on the diagonal. In the Appendix we show that after the measurement, the matrix with variances is given by $S'=S-W(\lambda,S)$, where $W(\lambda,S)$ is positive semidefinite. This means that after a measurement, the variances of the matrix elements decrease by an amount $W(\lambda,S)$, which only depends on the current variance matrix and the wavelength of a measurement, but not on the outcome of the measurement. So now we can plot the (square root of the) diagonal elements of the new variance matrix S' as a function of the wavelength, and see where the biggest reduction in the uncertainty of the dipole matrix elements occurs. The result is given in Fig. 3. As explained in the Appendix, the result is not reliable for $580<\lambda<610$ nm. In the light of the PNC experiments, we are especially interested in the $\langle 5D_{3/2}||D||6P_{1/2}\rangle$ matrix element,

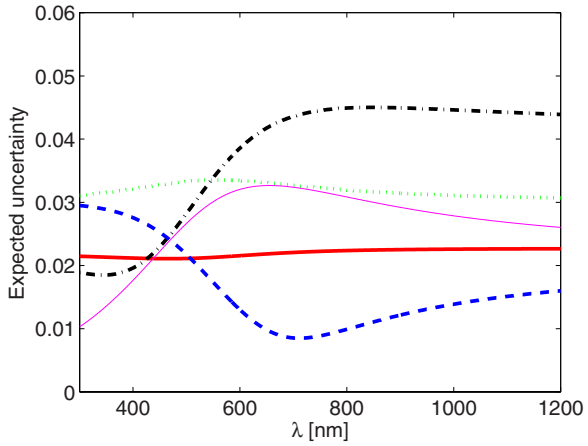

FIG. 3. (Color online) The expected uncertainties of the relevant matrix elements of Ba^+ after a measurement of the light-shift ratio at wavelength λ. In this plot, the information from the first two experiments has been taken into account. The following elements are plotted: $\langle 6S_{1/2}||D||6P_{1/2}\rangle$ (solid red line), $\langle 6S_{1/2}||D||6P_{3/2}\rangle$ (dotted green line), $\langle 5D_{3/2}||D||6P_{1/2}\rangle$ (dash-dotted black line), $\langle 5D_{3/2}||D||6P_{3/2}\rangle$ (dashed blue line), and $\langle 5D_{3/2}||D||4F_{5/2}\rangle$ (thin magenta line). To plot the elements in the same figure, we divided the $\langle 5D_{3/2}||D||4F_{5/2}\rangle$ uncertainty by a factor of 10.

p_7. Therefore, the best wavelength to perform a new ratio measurement would be around 350 nm. Provided it is accurate enough, such a measurement could reduce the uncertainty in this matrix element further from 0.05 down to 0.02.

V. DIPOLE MATRIX ELEMENTS FOR THE RADIUM ION

In the same way as for Ba^+, we have used the CCSD(T) method to calculate the dipole matrix elements of Ra^+. The results are shown in Table IV. The error bars of different matrix elements are estimated in the same way as for Ba^+. We also show the other available calculations [17,30,31]. Most of our results agree with them, up to the first decimal place. Using our theoretical values, we have calculated the transition probabilities and the lifetimes of the $7P_{1/2}$ and $7P_{3/2}$ states. These are given in Table V. Using the average of the theoretical values in Table IV, viz.,

$$p_1 = \langle 7S_{1/2}||D||7P_{1/2}\rangle = 3.25(3),$$

$$p_4 = \langle 7S_{1/2}||D||7P_{3/2}\rangle = 4.51(3),$$

$$p_7 = \langle 6D_{3/2}||D||7P_{1/2}\rangle = 3.58(4),$$

$$p_{10} = \langle 6D_{3/2}||D||7P_{3/2}\rangle = 1.52(2),$$

$$p_{13} = \langle 6D_{3/2}||D||5F_{5/2}\rangle = 4.56(16), \quad (5.1)$$

we have calculated the differential light shifts between the $m_{1/2}$ and $m_{-1/2}$ states of the $7S_{1/2}$ and $6D_{3/2}$ levels. The result is shown in Fig. 4. As the plot shows, the light shift of the D

TABLE V. The lifetimes of the $7P_{1/2}$ and $7P_{3/2}$ states of Ra^+. The probability coefficients A are given in MHz, and the lifetimes in ns.

$7P_{1/2}$		$7P_{3/2}$	
$A(\rightarrow 7S_{1/2})$	106.8(1.3)	$A(\rightarrow 7S_{1/2})$	188.0(3.8)
$A(\rightarrow 6D_{3/2})$	10.6(3)	$A(\rightarrow 6D_{3/2})$	3.4(1)
		$A(\rightarrow 6D_{5/2})$	22.9(1.8)
$A^{E1}(7P_{1/2})$	116.7(1.3)	$A^{E1}(7P_{1/2})$	214.2(4.2)
$\tau(7P_{1/2})$	8.57(10)	$\tau(7P_{3/2})$	4.67(9)

TABLE IV. Theoretical (absolute) values of the reduced dipole matrix elements of Ra^+. Estimated error bars are given inside parentheses.

Transition	Δλ (nm)		Present	Ref. [13]	Ref. [17]	Ref. [31]
$7S_{1/2}\rightarrow 7P_{1/2}$	468.358	p_1	3.28(2)	3.224	3.2545	3.254
$7S_{1/2}\rightarrow 8P_{1/2}$	197.605	p_2	0.04(4)	0.088		0.047
$7S_{1/2}\rightarrow 9P_{1/2}$		p_3	0.09(3)	0.116		
$7S_{1/2}\rightarrow 7P_{3/2}$	381.550	p_4	4.54(2)	4.477	4.5106	4.511
$7S_{1/2}\rightarrow 8P_{3/2}$	190.869	p_5	0.49(2)	0.339		0.395
$7S_{1/2}\rightarrow 9P_{3/2}$	157.703	p_6	0.30(2)	0.095		
$6D_{3/2}\rightarrow 7P_{1/2}$	1079.119	p_7	3.62(5)	3.550	3.5659	3.566
$6D_{3/2}\rightarrow 8P_{1/2}$	259.594	p_8	0.06(2)	0.013		0.049
$6D_{3/2}\rightarrow 9P_{1/2}$		p_9	0.02(1)	0.013		
$6D_{3/2}\rightarrow 7P_{3/2}$	707.991	p_{10}	1.54(2)	1.504	1.5117	1.512
$6D_{3/2}\rightarrow 8P_{3/2}$	248.092	p_{11}	0.15(2)	0.127		0.144
$6D_{3/2}\rightarrow 9P_{3/2}$	194.833	p_{12}	0.07(2)	0.057		
$6D_{3/2}\rightarrow 5F_{5/2}$	270.976	p_{13}	4.67(2)		4.4491	
$6D_{3/2}\rightarrow 5F_{5/2}$	210.832	p_{14}	0.86(4)			
$6D_{3/2}\rightarrow 5F_{5/2}$	183.697	p_{15}	0.48(11)			
$7P_{3/2}\rightarrow 5D_{5/2}$			4.83(8)	4.816	4.8232	

state goes through zero at a wavelength of 721 nm. Clearly visible again in the plot are the peaks at the different transitions. For the $7S_1/2$ state, these are the transitions to the $7P_{3/2}$ state at 382 nm, and to the $6P_{1/2}$ state at 468 nm. For the $6D_{3/2}$ state, we have at 271 nm the transition to the $5F_{5/2}$ state, at 708 nm the transition to the $7P_{3/2}$ state, and at 1080 nm the transition to the $7P_{1/2}$ state. Shown in the plot are the contributions from these different states to the total light shift.

Since Ra^+ has been proposed for PNC [3] and atomic clock [4] experiments, knowledge of the accuracies of the above $E1$ matrix elements are essential. This means that a similar measurement of the light-shift ratio in Ra^+ might be very useful. We will use the same method as for Ba^+ to find the optimal wavelength for such a measurement. We take as initial values the values in Eq. (5.1), where again the uncertainties are estimates. Figure 5 shows the attainable uncertainties using the current theoretical uncertainties, in order to assess good wavelengths for a light-shift ratio measurement in Ra^+. The results are not reliable for $710<\lambda<730$, as explained in the Appendix. Based on this figure, the most interesting wavelength for the $\langle 6D_{3/2}||D||7P_{1/2}\rangle$ matrix element is either around 500 nm or above the zero crossing at a wavelength of 750 nm.

VI. CONCLUSION

We have employed the relativistic coupled-cluster theory to calculate the electric dipole matrix elements in Ba^+ and Ra^+. Next, we have used the results of the recent measurement of the light-shift ratios in Ba^+ [20] to reduce the uncertainty of the most important matrix elements. Our recommended values are given in Eq. (4.2). These values agree with our CCSD(T) calculations to within 2 standard deviations. They result in $\tau(6P_{1/2})=7.92(10)$ ns and $\tau(6P_{3/2})=6.30(17)$ ns, in excellent agreement with experimental results. We further demonstrated that a new measurement of the light-shift ratio in Ba^+ around 350 nm could further reduce the uncertainty of the (for PNC studies, important) $\langle 5D_{3/2}||D||6P_{1/2}\rangle$ matrix element from 1.7% to 0.7%. For Ra^+, where no experimental data are available, we discussed what the most informative wavelength would be for a similar light-shift ratio measurement. For the $\langle 6D_{3/2}||D||7P_{1/2}\rangle$ (PNC) matrix element, a measurement of either around 500 or 750 nm would be optimal.

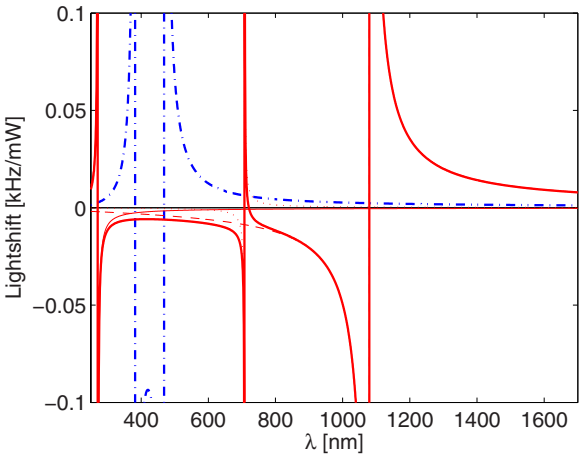

FIG. 4. (Color online) The differential light shifts between the $m_{1/2}$ and $m_{-1/2}$ states of the $7S_{1/2}$ (dash-dotted blue line) and $6D_{3/2}$ (thick solid red line) levels of Ra^+. We used the averaged theoretical results and assumed a laser focused on a spot with radius of 50 μm. Also shown are the individual contributions from $\langle 6D_{3/2}||D||7P_{1/2}\rangle$ (dashed red line), $\langle 6D_{3/2}||D||7P_{3/2}\rangle$ (dotted red line), and $\langle 6D_{3/2}||D||5F_{5/2}\rangle$ (thin red line).

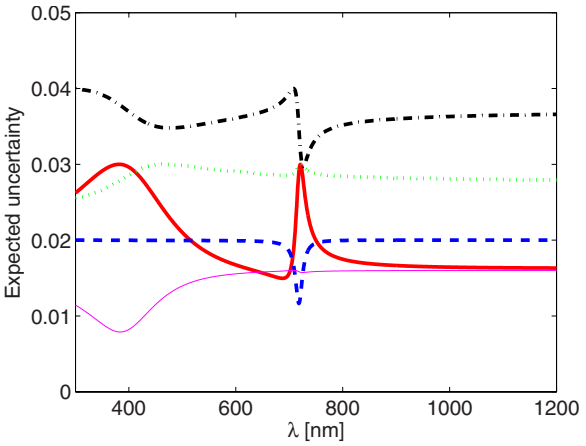

FIG. 5. (Color online) The expected uncertainties of the relevant matrix elements of Ra^+ after a measurement of the light-shift ratio at wavelength λ: $\langle 7S_{1/2}||D||7P_{1/2}\rangle$ (solid red line), $\langle 7S_{1/2}||D||7P_{3/2}\rangle$ (dotted green line), $\langle 6D_{3/2}||D||7P_{1/2}\rangle$ (dash-dotted black line), $\langle 6D_{3/2}||D||7P_{3/2}\rangle$ (dashed blue line), and $\langle 6D_{3/2}||D||5F_{5/2}\rangle$ (thin magenta line). To plot the elements in the same figure, we divided the $\langle 6D_{3/2}||D||5F_{5/2}\rangle$ uncertainty by a factor of 10.

ACKNOWLEDGMENTS

This work was supported by NWO under the VENI program with Project No. 680-47-128 and part of the Stichting FOM Physics Program 48 (TRIμP). We thank Norval Fortson, Jeff Sherman, Bhanu Pratap Das, Dmitry Budker, and Tom Wansbeek for useful discussions.

APPENDIX

We indicate the initial values of p by $\bar{p}$. We start by assuming that the matrix elements p are distributed normally,

$$p \sim \mathcal{N}(\bar{p},S),$$

where S is a 5×5 matrix with the variances of p_i on the diagonal. Next, we approximate $\mathcal{R}$ by a Taylor series around $p=\bar{p}$,

$$\mathcal{R}(\lambda;p) = \mathcal{R}(\lambda;\bar{p}) + (p-\bar{p})^T \cdot \left.\frac{\partial\mathcal{R}(\lambda;p)}{\partial p}\right|_{p=\bar{p}} + O(p^2)$$

$$\approx c + p^T \cdot \beta,$$

where

$$\beta = \beta(\lambda;\bar{p}) = \left.\frac{\partial \mathcal{R}(\lambda;p)}{\partial p}\right|_{p=\bar{p}},$$

and

$$c = c(\lambda;\bar{p}) = \mathcal{R}(\lambda;\bar{p}) - \bar{p}^T \cdot \left.\frac{\partial \mathcal{R}(\lambda;p)}{\partial p}\right|_{p=\bar{p}},$$

and T indicates the transpose. We are interested in the values of p, given that $\beta^T p + c = q$, where q is the measured value of the light-shift ratio. Using the properties of the conditional normal distribution [32] we find that

$$\begin{pmatrix} p \\ \beta^T p + c \end{pmatrix} \sim \mathcal{N}\left(\begin{pmatrix} \bar{p} \\ \beta^T \bar{p} + c \end{pmatrix}, \begin{pmatrix} S & S\beta \\ \beta^T S & \beta^T S \beta \end{pmatrix}\right),$$

which leads to

$$p|(\beta^T p + c = q) \sim \mathcal{N}(\bar{p} + S\beta(\beta^T S\beta)^{-1}(q - c - \beta^T \bar{p}), S - W),$$

with $W = W(\lambda, S) \equiv S\beta(\beta^T S\beta)^{-1}\beta^T S$, a positive semidefinite matrix.

The above formula can be interpreted as follows. The initial values $\bar{p}$ of the matrix elements are, due to the outcome of the ratio measurement, changed by an amount $S\beta(\beta^T S\beta)^{-1}(q - c - \beta^T \cdot \bar{p})$. More interestingly, however, the variance of the matrix elements is reduced by a factor of $W(\lambda, S)$. Since W is a function of the wavelength λ and does not depend on the outcome of the measurement (provided it is "accurate enough"), we can use it to find that wavelength at which a measurement of the ratio gives the largest reduction in the variance.

The accuracy of this approach depends of course on the accuracy of the Taylor approximation. We found that the linear fit is a very good approximation (better than 2%), except in the region where the light-shift ratio goes through zero. For Ba^+, this means that in the narrow window $580 < \lambda < 610$ nm, our method is not reliable. For Ra^+, the method fails between 710 and 730 nm.

[1] N. Fortson, Phys. Rev. Lett. **70**, 2383 (1993).
[2] T. W. Koerber, M. Schacht, W. Nagourney, and E. N. Fortson, J. Phys. B **36**, 637 (2003).
[3] L. W. Wansbeek, B. K. Sahoo, R. G. E. Timmermans, K. Jungmann, B. P. Das, and D. Mukherjee, Phys. Rev. A **78**, 050501(R) (2008).
[4] B. K. Sahoo, B. P. Das, R. K. Chaudhuri, D. Mukherjee, R. G. E. Timmermans, and K. Jungmann, Phys. Rev. A **76**, 040504(R) (2007).
[5] B. K. Sahoo, B. P. Das, R. K. Chaudhuri, and D. Mukherjee, Phys. Rev. A **75**, 032507 (2007).
[6] W. M. Itano, J. Res. Natl. Inst. Stand. Technol. **105**, 829 (2000).
[7] A. Kastberg, P. Villemoes, A. Arnesen, F. Heijkenskjöld, A. Langereis, P. Jungner, and S. Linnaeus, J. Opt. Soc. Am. B **10**, 1330 (1993).
[8] J. Reader, C. H. Corliss, W. L. Wiese, and G. A. Martin, *Wavelengths and Transition Probabilities for Atoms and Atomic Ions*, Natl. Bur. Stand. (U.S.) Circ. No. 68 (U.S. GPO, Washington, D.C., 1980), Vol. X.
[9] A. Gallagher, Phys. Rev. **157**, 24 (1967).
[10] P. Kuske, N. Kirchner, W. Wittmann, H. J. Andrä, and D. Kaiser, Phys. Lett. **64A**, 377 (1978).
[11] E. H. Pinnington, R. W. Berends, and M. Lumsden, J. Phys. B **28**, 2095 (1995).
[12] H. J. Andrä, *Beam-Foil Spectroscopy 2* (Plenum, New York, 1976).
[13] V. A. Dzuba, V. V. Flambaum, and J. S. M. Ginges, Phys. Rev. A **63**, 062101 (2001).
[14] G. Gopakumar, H. Merlitz, R. K. Chaudhuri, B. P. Das, U. S. Mahapatra, and D. Mukherjee, Phys. Rev. A **66**, 032505 (2002).
[15] E. Iskrenova-Tchoukova and M. S. Safronova, Phys. Rev. A **78**, 012508 (2008).
[16] C. Guet and W. R. Johnson, Phys. Rev. A **44**, 1531 (1991).
[17] U. I. Safronova, W. R. Johnson, and M. S. Safronova, Phys. Rev. A **76**, 042504 (2007).
[18] T. Koerber, Ph.D. thesis, University of Washington, 2003 (unpublished).
[19] J. A. Sherman, T. W. Koerber, A. Markhotok, W. Nagourney, and E. N. Fortson, Phys. Rev. Lett. **94**, 243001 (2005).
[20] J. A. Sherman, A. Andalkar, W. Nagourney, and E. N. Fortson, Phys. Rev. A **78**, 052514 (2008).
[21] K. D. Bonin and V. V. Kresin, *Electric-Dipole Polarizabilities of Atoms, Molecules and Clusters* (World Scientific, Singapore, 1997).
[22] P. Rosenbusch, S. Ghezali, V. A. Dzuba, V. V. Flambaum, K. Beloy, and A. Derevianko, Phys. Rev. A **79**, 013404 (2009).
[23] B. K. Sahoo, S. Majumder, R. K. Chaudhuri, B. P. Das, and D. Mukherjee, J. Phys. B **37**, 3409 (2004).
[24] F. Parpia, C. Froese Fischer, and I. P. Grant (unpublished).
[25] B. P. Das (private communication).
[26] J. J. Curry and NIST team, J. Phys. Chem. Ref. Data **33**, 725 (2004).
[27] J. Klose, J. Fuhr, and W. Wiese, J. Phys. Chem. Ref. Data **31**, 217 (2002).
[28] M. D. Davidson, L. C. Snoek, H. Volten, and A. Doenszelmann, Astron. Astrophys. **255**, 457 (1992).
[29] N. Kurz, M. R. Dietrich, G. Shu, R. Bowler, J. Salacka, V. Mirgon, and B. B. Blinov, Phys. Rev. A **77**, 060501(R) (2008).
[30] V. A. Dzuba, V. V. Flambaum, and M. S. Safronova, Phys. Rev. A **73**, 022112 (2006).
[31] R. Pal, D. Jiang, M. S. Safronova, and U. I. Safronova, e-print arXiv:0901.4195.
[32] T. Anderson, *An Introduction to Multivariate Statistical Analysis* (Wiley, New York, 1958).